# Choline-releasing glycerophosphodiesterase EDI3 drives tumor cell migration and metastasis

Joanna D. Stewart[a,1], Rosemarie Marchan[a,1], Michaela S. Lesjak[a], Joerg Lambert[b], Roland Hergenroeder[b], James K. Ellis[c], Chung-Ho Lau[c], Hector C. Keun[c], Gerd Schmitz[d], Juergen Schiller[e], Mandy Eibisch[e], Christian Hedberg[f], Herbert Waldmann[f,g], Ekkehart Lausch[h], Berno Tanner[i], Jalid Sehouli[j], Jens Sagemueller[k], Hagen Staude[l], Eric Steiner[m,2], and Jan G. Hengstler[a,2,3]

[a]Leibniz Research Centre for Working Environment and Human Factors (IfADO), University of Dortmund, 44139 Dortmund, Germany; [b]Interface Processes, Leibniz-Institut fuer Analytische Wissenschaften (ISAS), 44227 Dortmund, Germany; [c]Biomolecular Medicine, Department of Surgery and Cancer, Faculty of Medicine, Imperial College London, London SW7 2AZ, United Kingdom; [d]Institute for Clinical Chemistry and Laboratory Medicine, University Hospital Regensburg, 93053 Regensburg, Germany; [e]Medical Faculty, Institute of Medical Physics and Biophysics, University of Leipzig, 04107 Leipzig, Germany; [f]Chemical Biology, Max Planck Institute of Molecular Physiology, 44227 Dortmund, Germany; [g]Fakultaet Chemie, Lehrbereich Chemische Biologie, Technische Universitaet Dortmund, 44227 Dortmund, Germany; [h]Department of Pediatrics, Freiburg University Medical Center, 79106 Freiburg, Germany; [i]Department of Obstetrics and Gynecology, Oranienburg Clinic, 16515 Oranienburg, Germany; [j]Department of Gynecology, Charite University Hospital, 13353 Berlin, Germany; [k]Department of Pharmacy, Duesseldorf University Hospital, 40225 Duesseldorf, Germany; [l]Department of Pediatrics, University of Rostock, 18057 Rostock, Germany; and [m]Department of Obstetrics and Gynecology, Gesundheits-und Pflegezentrum Ruesselsheim Gemeinnützige GmbH, 65428 Ruesselsheim, Germany

Edited by Dennis A. Carson, University of California at San Diego, La Jolla, CA, and approved April 4, 2012 (received for review October 26, 2011)

**Metastasis from primary tumors remains a major problem for tumor therapy. In the search for markers of metastasis and more effective therapies, the tumor metabolome is relevant because of its importance to the malignant phenotype and metastatic capacity of tumor cells. Altered choline metabolism is a hallmark of cancer. More specifically, a decreased glycerophosphocholine (GPC) to phosphocholine (PC) ratio was reported in breast, ovarian, and prostate cancers. Improved strategies to exploit this altered choline metabolism are therefore required. However, the critical enzyme cleaving GPC to produce choline, the initial step in the pathway controlling the GPC/PC ratio, remained unknown. In the present work, we have identified the enzyme, here named EDI3 (endometrial differential 3). Purified recombinant EDI3 protein cleaves GPC to form glycerol-3-phosphate and choline. Silencing EDI3 in MCF-7 cells decreased this enzymatic activity, increased the intracellular GPC/PC ratio, and decreased downstream lipid metabolites. Downregulating EDI3 activity inhibited cell migration via disruption of the PKCα signaling pathway, with stable overexpression of EDI3 showing the opposite effect. EDI3 was originally identified in our screening study comparing mRNA levels in metastasizing and nonmetastasizing endometrial carcinomas. Both Kaplan–Meier and multivariate analyses revealed a negative association between high EDI3 expression and relapse-free survival time in both endometrial ($P < 0.001$) and ovarian ($P = 0.029$) cancers. Overall, we have identified EDI3, a key enzyme controlling GPC and choline metabolism. Because inhibition of EDI3 activity corrects the GPC/PC ratio and decreases the migration capacity of tumor cells, it represents a possible target for therapeutic intervention.**

glycerophosphodiesterase 5 | phosphatidic acid | lysophosphatidic acid | glycerophosphocholine phosphodiesterase GDE1 homolog (*Saccharomyces cerevisiae*) | glycerophosphodiester phosphodiesterase domain containing 6

It is widely accepted that choline metabolism represents a critical aspect of the tumor metabolome (1–4). As cells undergo malignant transformation, there is an overall increase in total choline metabolites and phosphocholine (PC). The elevation of PC and total choline is increasingly used in tumor diagnostics with detection by $^{1}H$ or $^{31}P$ magnetic resonance spectroscopy (5–9). In breast and ovarian carcinomas, elevated PC are accompanied by a decrease in glycerophosphocholine (GPC), resulting in a decreased GPC/PC ratio compared with normal tissue (1, 4). The increased PC levels have previously been reported to occur through several mechanisms; however, the decreased GPC has not yet been adequately explained.

Choline kinase (CK) is the enzyme responsible for the phosphorylation of available intracellular choline to PC, and is active in malignant cells and tumors of lung, colon, breast, cervix, and ovary (4, 7, 10–12). Targeting CK with inhibitors resulted in antimitogenic and antiproliferative effects (13). It has also been reported that an increased rate of choline transport may be responsible for the increased PC levels (10, 14, 15). However, gene-expression analysis of members of the three choline transporter families in ovarian cancer cells showed no differential levels for the high-affinity transporter families compared with normal cells (7). A further source of choline is through an increase in phospholipase D (PLD) activity (16, 17). PLD is a phospholipase that hydrolyses phosphatidylcholine (PtdCho) to phosphatidic acid (PA) and choline. Increased PLD expression and activity was reported in the metastatic breast cancer cell line, MDA-MB-231, and inhibition of activity in these cells rendered them more sensitive to apoptotic insult (17).

At present, the only reported mechanism that involves GPC is the report of increased phospholipase A2 ($PLA_2$) activity (18). $PLA_2$ is a membrane associated phospholipase, which hydrolyses the sn-2 fatty acyl ester bond of phosphoglycerides, converting PtdC to 1-acylglycerophosphocholine, a precursor to GPC. Membrane $PLA_2$ enzyme levels were significantly higher in breast cancer patients with distant metastases compared with patients without metastases (19).

In this study we provide a direct mechanism for the decreased GPC levels observed in various cancer cells and tissues. Increased expression and activity of endometrial differential 3 (EDI3), the enzyme responsible for the cleavage of GPC, does not only provide a source of choline for the Kennedy pathway, resulting in increased PC, but also directly explains the decreased GPC levels reported in transformed cells (1, 4). Because GPC is a key component of choline metabolism, we used both NMR and mass spectrometry to investigate the role of EDI3 in lipid metabolism and in particular the GPC/PC ratio. We further

Author contributions: J.D.S., R.M., E.S., and J.G.H. designed research; J.D.S., R.M., M.S.L., J.L., J.K.E., C.-H.L., and M.E. performed research; R.H., J.K.E., H.C.K., G.S., J. Schiller, C.H., H.W., E.L., B.T., J. Sehouli, J. Sagemueller, H.S., and E.S. contributed new reagents/analytic tools; J.D.S., R.M., M.S.L., J.L., J.K.E., G.S., J. Schiller, and C.H. analyzed data; and J.D.S., R.M., and J.G.H. wrote the paper.

The authors declare no conflict of interest.

This article is a PNAS Direct Submission.

Freely available online through the PNAS open access option.

[1]J.D.S. and R.M. contributed equally to this work.

[2]E.S. and J.G.H. contributed equally to this work.

[3]To whom correspondence should be addressed. E-mail: Hengstler@ifado.de.

This article contains supporting information online at www.pnas.org/lookup/suppl/doi:10.1073/pnas.1117654109/-/DCSupplemental.

examined the impact of EDI3 expression on signaling pathways known to be involved in cellular migration.

## Results

**EDI3 Predicts Metastasis in Endometrial and Ovarian Cancer.** A screening set of endometrial carcinomas consisting of pairs of tumor tissue specimens with identical histopathological features but different metastatic behavior were used to identify differentially expressed genes by differential display analysis. A 270-bp fragment was found only in the tumors that went on to form metastasis. Furthermore, higher expression of this gene, named *EDI3*, was confirmed in metastasizing carcinomas by quantitative RT-PCR (qRT-PCR) using an independent cohort ($P < 0.001$) (Fig. 1*A*, using alternative primers in Fig. S1*A*, and Table S1). Both Kaplan–Meier and multivariate analyses revealed a negative association between high *EDI3* expression and relapse-free survival time in endometrial cancer independent of classic prognostic factors, such as Federation of Gynecology and Obstetrics (FIGO) stage, tumor grade, depth of myometrial invasion, diabetes mellitus, or age (Fig. 1 *B* and *C*, and Fig. S1 *B* and *C*). Taken together, these data suggest *EDI3* expression could be a valuable marker for metastatic potential in endometrial cancers and, therefore, aid clinical decisions. An association of *EDI3* with worse prognosis was also obtained in a cohort of patients with ovarian cancer, suggesting a more general role in cancer pathology (Fig. 1*D* and Table S2).

**EDI3 Is a GPC Phosphodiesterase.** Analysis of the 270-bp differential display sequence confirmed 99% homology to the *GPCPD1*, GPC phosphodiesterase (PDE) GDE1 (*Saccharomyces cerevisiae*) homolog gene on chromosome 20p13. Glycerophosphocholine phosphodiesterase GDE1 homolog (*Saccharomyces cerevisiae*) (GPCPD1) is included as a member of the mammalian glycerophosphodiesterase (GDE) family (20), specifically GDE5, because of the presence of a GDE domain at the N terminus. Unlike other members of the GDE family, GDE5/GPCPD1/EDI3 (EDI3 for simplicity) contains no transmembrane domains, but is instead localized to the cytoplasm (20, 21). A recent study illustrated that the preferred substrate for EDI3 is GPC, and that in mice the enzyme may play an important role in skeletal muscle development (21). However, the presence of *EDI3* mRNA in all tissues of both mouse and human (Fig. S1 *D* and *E*) suggests a more generalized physiological function.

To specifically investigate the enzymatic action of EDI3, high-resolution $^{31}$P NMR analyses were performed using GPC as a substrate. Incubating lysates from EDI3 overexpressing NIH 3T3 cells resulted in a time-dependent increase in glycerol-3-phosphate (G3P) signal (Fig. 2*A*). Similar results were obtained with recombinant EDI3 protein (Fig. 2*B*), confirming that EDI3 hydrolyses GPC to form G3P. The presence of the second cleavage product, choline, was confirmed using a modified enzyme-coupled spectrophotometric assay. A significant increase in choline production was measured in lysates from NIH 3T3 cells overexpressing human EDI3 when incubated with GPC (Fig. 2*C*). Conversely, knocking down EDI3 in MCF-7 and AN3-CA cells using siRNA (Fig. S2 *A*–*C*) significantly decreased choline formation (Fig. 2*D* and Fig. S2*D*). Furthermore, incubating GPC with increasing concentrations of EDI3 recombinant protein resulted in a concentration-dependent increase in choline production (Fig. 2*E*). The enzyme kinetics of EDI3 were calculated as $K_m$ 3.87 ± 0.84 × $10^{-4}$ M and $V_{max}$ 15.8 ± 2 $nMS^{-1}$.

It is well accepted that GPC can be cleaved to form G3P and choline; however, the gene coding the enzyme responsible for this reaction remained unclassified (E.C.3.1.4.2). Our results demonstrate that EDI3 is the enzyme responsible for cleavage of GPC in mammalian cells, providing two key molecules important for various phospholipid signaling pathways, such as choline for the first step in the Kennedy pathway. GDE2 [glycerophosphodiester phosphodiesterase domain containing 5 (GDPD5)] is the only other enzyme family member reported to metabolize GPC (22).

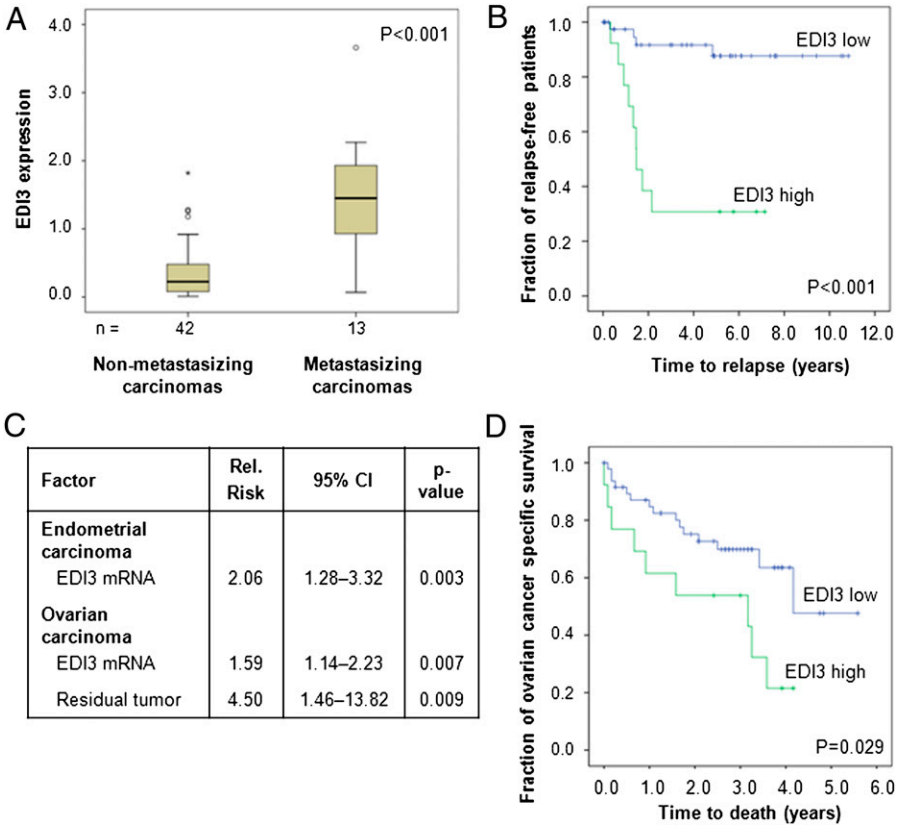


| Factor | Rel. Risk | 95% CI | p-value |
|---|---|---|---|
| Endometrial carcinoma | | | |
| EDI3 mRNA | 2.06 | 1.28–3.32 | 0.003 |
| Ovarian carcinoma | | | |
| EDI3 mRNA | 1.59 | 1.14–2.23 | 0.007 |
| Residual tumor | 4.50 | 1.46–13.82 | 0.009 |

**Fig. 1.** *EDI3* expression is associated with worse prognosis in endometrial and ovarian cancer. (*A*) Higher mRNA expression of *EDI3* in metastasizing compared with nonmetastasizing primary endometrial carcinomas. The top of the box represents the 75th percentile, the bottom represents the 25th percentile, and the middle line represents the 50th percentile. The whiskers (the lines that extend out the top and bottom of the box) represent the highest and lowest values that are not outliers or extreme values. The circles represent the outliers (values that are between 1.5 and 3 times the interquartile range), and the asterisk represents an extreme value (one that is more than 3 times the interquartile range). (*B*) High *EDI3* expression is associated with shorter time to relapse in endometrial cancer. (*C*) *EDI3* is prognostic in multivariate analysis independent from established clinical factors. The Cox analysis of endometrial cancer was adjusted to FIGO stage (I and II vs. III and IV), grading (G1, G2 vs. G3), depth of invasion (0–2 mm vs. >3 mm), age (younger versus older than 70 y), and diabetes mellitus. The latter factors were not included as significant into the Cox model. Ovarian cancer was adjusted to age (older vs. younger than 55 y), residual tumor after surgery (present vs. not present), tumor stage (FIGO III and IV vs. I and II), grade (G1 vs. G2, G3), and histological type (serous vs. nonserous). Of the latter factors only residual tumor was accepted as significant by the model. (*D*) High *EDI3* expression is associated with shorter survival in epithelial ovarian cancer.

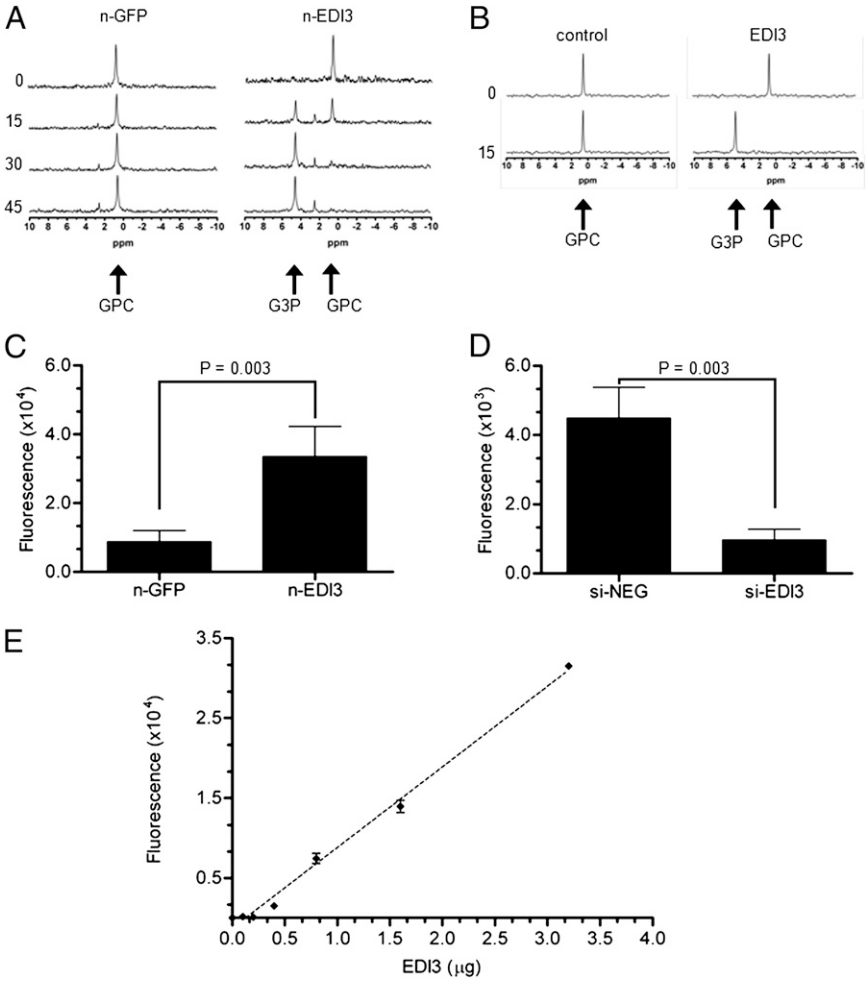


**Fig. 2.** EDI3 is a GPC PDE. (*A*) Protein lysates from NIH 3T3 vector control cells (n-GFP) or cells stably overexpressing EDI3 (n-EDI3) were incubated with GPC for 15, 30, or 45 min. Samples were then analyzed using $^{31}$P-NMR to determine the presence of GPC (0.6 ppm) and G3P (4.5 ppm). Both samples show a small peak at 2.4 ppm, representing inorganic phosphate (Pi), which slowly increases with incubation time (GPC/Pi ratio = 0.138 ± 0.116). In the n-EDI3 cell lysate, the ratio of G3P to GPC dramatically increased over time: 0.969, 11.83, and 17.63 at 15, 30, and 45 min, respectively. (*B*) Recombinant EDI3 protein was incubated with GPC for 15 min, and the samples were then analyzed using $^{31}$P-NMR. A clear shift from the substrate GPC peak at 0.6 ppm to the product G3P at 4.5 ppm is observed. (*C*) Enzyme-coupled spectrophotometric assay showing choline production from GPC upon incubation of NIH 3T3 vector control cell lysate (n-GFP) or cell lysate from stably overexpressing EDI3 cells (n-EDI3). (*D*) Enzyme-coupled spectrophotometric assay showing choline release from GPC upon incubation of MCF-7 cell lysates treated with scrambled siRNA (si-NEG) or EDI3 siRNA (si-EDI3). (*E*) Enzyme-coupled spectrophotometric assay showing recombinant EDI3 releases choline from GPC in a concentration dependent manner. Values in graphs *C–E* represent mean ± SD from three independent experiments. Student *t* test was used for all statistical analysis.

Recently Cao et al. reported that GDE2 may be the enzyme responsible for the GPC cleavage and altered choline metabolism observed in breast cancer tumors (23). However, their conclusion was that the expression of GDE2 was not enough to explain the altered GPC levels observed (23). In our cell lines, knocking down EDI3 did not alter *GDE2* mRNA levels (Fig. S2*E*), suggesting that GDE2 did not compensate for, or contribute to, the phenotype observed through the silencing of EDI3. Accordingly, cleavage of GPC occurs primarily by EDI3 and may result in increased PC and malignant transformation (Fig. 3*A*).

**EDI3 Expression Alters Choline Metabolism.** We investigated the endogenous levels of both GPC and PC using high-resolution $^{1}$H NMR in MCF-7 cells with decreased EDI3 expression. Cells treated with scrambled siRNA showed the characteristic low GPC/PC ratio (GPC/PC = 0.2), as previously reported in breast cancer cell lines (1). Knockdown of EDI3 increased GPC levels and decreased PC levels to give an increased ratio of 0.6, implying a switch toward an untransformed phenotype (Fig. 3*B* and Fig. S3) (1–4). EDI3's influence on GPC and PC levels was also confirmed in MDA-MB-231 and AN3-CA cells (Figs. S2*F* and S3 *A* and *B*). GPC levels were more profoundly affected than PC levels after EDI3 knockdown (in all cell lines), confirming that EDI3's direct action is on GPC.

To analyze if EDI3-mediated alterations in GPC and PC levels influence downstream lipid metabolites, we quantified PtdCho, PA, and lysophosphatidic acid (LPA) using mass spectrometry. Although no significant alterations were observed for PtdCho, both PA and LPA levels significantly decreased in EDI3 siRNA cells relative to control cells (Fig. 3*C*), suggesting disruptions to metabolic pathways downstream of EDI3. Previous studies have shown that the activity of CK, which generates PC from choline, is increased in cancer cells (4, 7, 10–12). EDI3 acts upstream of CK, adding further evidence that disruption of this metabolic pathway can play a significant role in tumor progression.

**EDI3 Positively Regulates Cell Migration in Vitro via PKCα Signaling.** Transformation of a normal cell to a tumor cell is hallmarked by several phenotypic and genetic changes, as reviewed and revised by Hanahan and Weinberg (24). Analysis using the classic scratch assay showed that decreasing EDI3 caused a clear delay in wound closure in both MCF-7 and AN3-CA cells (Fig. 4*A* and Fig. S4*A*). Accordingly, overexpressing EDI3 in MCF-7 cells (Fig. S4*B*) increased the rate at which cells closed the gap (Fig. 4*B*). The observed effects on the scratch assay are a result of altered migration, not proliferation, as changing EDI3 expression did not cause a significant effect on the S phase of the cell cycle, nor was there any change in proliferating cell nuclear antigen expression after altering EDI3 expression (Fig. S4 *C–E*). The influence of EDI3 on migration was further confirmed using the highly metastatic MDA-MB-231 breast cancer cell line in the migration-specific Transwell chamber assay (Fig. 4*C*). Direct analysis of MDA-MB-231 cells by time-lapse microscopy also confirmed reduced migration after EDI3 knockdown (Movie S1).

To address whether the effect of EDI3 on migration depends on its PDE activity, we screened for chemical inhibitors of EDI3 using the enzyme-coupled spectrophotometric assay (Fig. S5*A*). Dipyridamole, a PDE5 inhibitor (25), significantly blocked EDI3

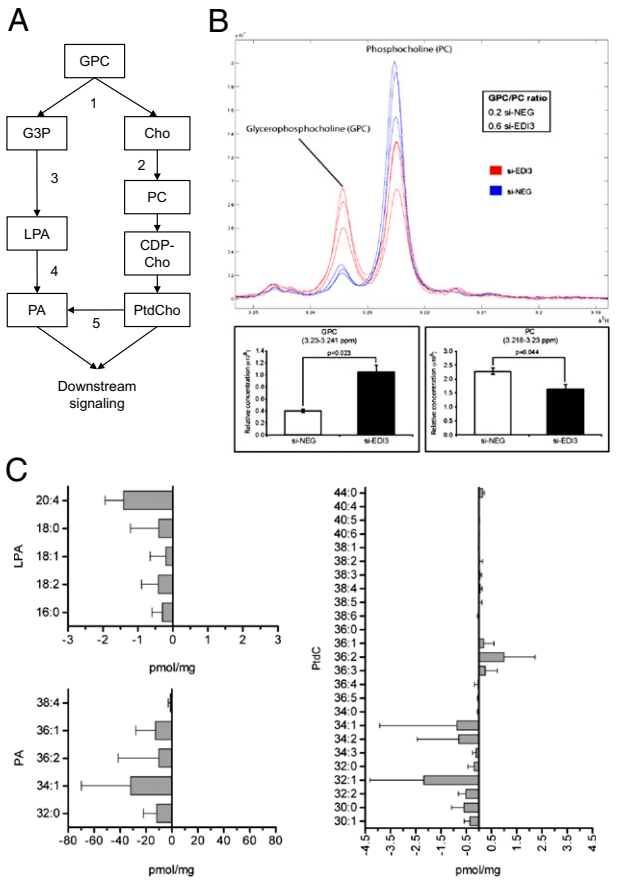


**Fig. 3.** EDI3 activity alters the choline metabolism pathway. (*A*) Simplified overview of choline metabolism outlining the Kennedy pathway and the formation of lipid second messengers, PA and LPA, which can activate downstream signaling proteins. Cho, choline; CDP-Cho, cytidine diphosphate-choline. Enzyme key: 1-EDI3, 2-choline kinase, 3-G3P acyltransferase, 4-LPA acyltransferase, 5-phospholipase D. (*B*) MCF-7 cells transfected with EDI3 siRNA (si-EDI3) caused an increase in the GPC/PC ratio, compared with scrambled siRNA (si-NEG), as demonstrated by $^{1}$H NMR spectroscopy. Bar graphs are mean ± SEM values of the relative concentration of GPC and PC. (*C*) Difference in cellular concentrations of PtdCho, PA, and LPA in MCF-7 cells transfected with EDI3 siRNA compared with those transfected with scrambled siRNA, measured using mass spectrometry. The differences for LPA ($P$ = 0.0056) and PA ($P$ = 0.0009) were significant, whereas for PtdCho only a nonsignificant trend was observed ($P$ = 0.101).

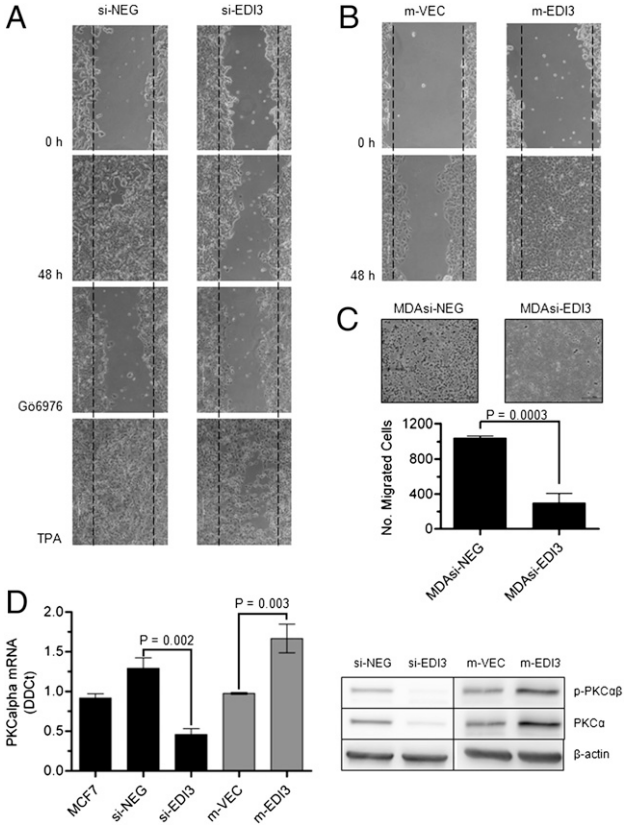


**Fig. 4.** EDI3 positively regulates cell migration via PKCα signaling in vitro. (*A*) Representative images of MCF-7 scratch assay for cells transfected with scrambled (si-NEG) or EDI3 siRNA (si-EDI3), either alone or in the presence of 3 μM Gö6976 or 1 mM TPA. (*B*) Representative images of MCF-7 scratch assay for vector control cells (m-VEC) or cells stably overexpressing EDI3 (m-EDI3). (*C*) Transwell migration assay using MDA-MB-231 cells transfected with scrambled (MDAsi-NEG) or EDI3 siRNA (MDAsi-EDI3). (*D*) mRNA and Western blot analysis of PKCα in MCF-7 cells. Cells were transfected with scrambled siRNA (si-NEG) or EDI3 siRNA (si-EDI3) or else stably transfected with vector control (m-VEC) or a vector overexpressing EDI3 (m-EDI3). Values in graphs *C* and *D* represent mean ± SD from three independent experiments. Student *t* test was used for all statistical analysis. Images for *A*, *B*, and *D* were taken with a 10× objective.

activity, but a second PDE5 inhibitor, Sildenafil (25), showed no effect. Tested under identical conditions in the scratch assay, only Dipyridamole was able to decrease the migration of MCF-7 cells, providing additional evidence that the cleavage of GPC by EDI3 is essential for migration (Fig. S5*B*).

The precise rationale for the high levels of PC in cancer is still not well understood (26). Choline metabolism not only provides membrane phospholipids essential for neoplastic cells, but is essential for the production and activation of a number of lipid second messengers and downstream signaling proteins (27, 28). Both LPA and PA (Fig. 3*A*) are known to activate the MAPK and PI3K signaling pathways (29–31), and inhibition of CK in cells was shown to significantly decrease both pAKT and pERK levels (26). However, EDI3 knockdown in MCF-7 cells showed no effect on either pathway (Fig. S6*A*). Choline metabolism is also known to activate the PKC signaling pathway (32). EDI3 siRNA in MCF-7 and AN3-CA cells decreased both RNA and protein levels of PKCα, with the opposite observed in MCF-7 cells overexpressing EDI3 (Fig. 4*D* and Fig. S6*B*). EDI3 had no effect on phosphorylation status or total levels of other PKC family members (Fig. S6*C*), nor on other proteins known to be involved in migration, including p38, c-jun, and SAPK/JNK (Fig. S6*D*). Activation or inhibition of PKCα with 12-*O*-tetradecanoylphorbol-13-acetate (TPA) or Gö6976, respectively, caused increased or decreased wound closure in control cells (Fig. 4*A*). In cells with EDI3 siRNA, TPA was able to rescue wound closure, whereas Gö6976 further increased the time taken to close the gap (Fig.4*A*). Furthermore, knocking down PKCα in the EDI3 overexpressing MCF-7 cells countered the increased rate of wound closure observed with EDI3 overexpression to that observed in the control cells (Fig. S6*E*). Taken together, the results show that EDI3 impacts cellular migration via PKCα signaling.

## Discussion

Aberrant choline metabolism is a common feature in cancer (1–4). Accordingly, the enzymes involved may play an important role in cancer progression. It has been well reported that malignant cells have increased PC levels, with several types of cancer reporting a switched GPC/PC ratio (1–4). Currently, only limited data are available on the enzymatic action of the protein encoded by the *EDI3* gene (21). In this study we show that EDI3 encodes a GPC PDE, which cleaves GPC to produce choline and G3P, thus providing choline for the Kennedy pathway and G3P

for downstream metabolic pathways. Our findings further show that silencing of EDI3 in MCF-7, MDA-MB-231, and AN3-CA cells, which have a low GPC/PC ratio typical of several tumor cell lines, caused a switch to a high GPC/PC ratio.

Furthermore, decreased expression of EDI3 in MCF-7 cells caused a subsequent decrease in lipid metabolites, PA and LPA. Both molecules can be produced by several pathways, for example the acylation of G3P to LPA, which is then converted to PA by a second acylation step. Alternatively, PA is formed from the hydrolysis of PtdCho by PLD. Activity and expression of PLD have been associated with worse prognosis in several cancers, and inhibitors against PLD are being designed as therapeutic agents (33). Although total PtdCho was not significantly altered after EDI3 down-regulation, we cannot exclude the possibility that specific pools of PtdCho were affected, as seen for shorter chain PtdCho species that did decrease after EDI3 knockdown. Additionally, it was previously shown the fatty acid composition of PtdCho rather than the PtdCho content itself was changed in prostate cancer tissue compared with benign prostatic hyperplasia (34). Both PA and LPA are important signaling molecules known to be involved in cellular transformation and several cancer types (30, 31, 35). LPA and PA have both been reported to activate PKC signaling, which we have shown to be altered after EDI3 silencing. PKCα has previously been associated with the proliferation, migration, and invasion of tumor cells (36–38). The observation that EDI3 silencing decreases migration through the PKCα signaling pathway may have important implications for understanding the role of EDI3 in metastasis. Although the relevance of EDI3 for the migration phenotype has been confirmed, it still has to be analyzed as to which of the downstream pathways (CK vs. GPAM) is most relevant.

The initial aim of this study was to identify and characterize genes associated with metastasis in endometrial cancer. We first examined the differential display of genes in metastasizing and nonmetastasizing endometrial carcinomas. Cancer of the endometrium is the most common malignancy of the female genital tract. The majority of endometrial carcinomas (69%) are diagnosed early and result in a high 5-y survival rate of more than 80%. However, patients who present with distant metastasis see this figure decrease to 17% (39). After complete tumor resection, survival usually depends on occurrence of metastasis at sites that include the para-aortic lymph nodes, bone, lung, pelvis, liver, and vagina (40). Currently, predicting the likelihood of metastasis in endometrial cancer remains challenging. Therefore, understanding the process that determines metastatic potential could provide new prognostic tools. The present study identified the gene *EDI3*, and showed that high expression is associated with worse prognosis in both endometrial and ovarian cancers. The significance of EDI3 in other cancer types remains to be elucidated.

Taken together, our findings indicate an important role for EDI3 in lipid metabolism and that aberrant expression may play a role in malignant transformation. We show that the effect on migration occurs through the PKCα signaling pathway, most likely through the activation of downstream metabolites. Although cells are supplied with choline by several pathways, the EDI3 mechanism is not fully compensated by alternatives and is therefore a critical enzymatic step. Our identification of EDI3 as a key factor of tumor cell migration may also provide a promising target for novel therapeutic strategies.

## Materials and Methods

**Clinical Specimens.** Patients with histologically proven endometrial cancer were collected at the Department of Obstetrics and Gynecology at the University Hospital in Mainz, Germany. Ovarian cancer samples were obtained from the ovarian cancer tumor bank at the Charite University Hospital in Berlin. Details are given in *SI Materials and Methods* and Tables S1 and S2. See Table S3 for a list of the T and P primers used in the study.

**Cell Culture.** MCF-7, MDA-MB-231, and AN3-CA cells were purchased from the German Collection of Microorganisms and Cell Cultures and maintained according to the suppliers' instructions. The authenticity of cells was confirmed by DNA fingerprinting by the German Resource Centre for Biological Material (DSMZ). MCF-7 cells, stably transfected with pCMV6-AC-GFP or pCMV6-AN-GFP-EDI3 were purchased from AMS Bio and maintained in DMEM with 10% (vol/vol) FCS, and 10 μg/mL insulin (Sigma), and 0.6 mg/mL G418 (Sigma). NIH 3T3 cells stably expressing pBABE-GFP (vector control) or pBABE-GFP-EDI3 with a V5 tag to overexpress human EDI3 were kindly provided by E.L. and maintained in DMEM supplemented with 10% (vol/vol) FCS (PAN Biotech) and 5 mg/mL penicillin/streptomycin (PAN Biotech).

**mRNA Expression.** Total RNA from cells or C57BL/6 mouse tissue was isolated using chloroform extraction and ethanol precipitation, or Qiagen's RNeasy Mini kit following the manufacturer's instructions. A human total RNA master panel (Clontech) was used to determine *EDI3* expression in human tissue. Two micrograms total RNA was transcribed into cDNA using the high-capacity cDNA Reverse Transcription Kit (Applied Biosystems). Quantitative PCR analysis was performed using Quantitect SYBR Green RT-PCR kit (Qiagen), custom-designed Quantitect primer assays [EDI3: QT00066598; β-actin: QT01680476; PKCα: QT00095746; GDPD5 (GDE2): QT00079716; TATA box binding protein: QT00000721; 18S: QT00199367] and the ABI 7500 Fast Real-Time PCR system (Applied Biosystems) according to the manufacturer's (Qiagen) instructions. Relative quantification was calculated using the $2^{-\Delta\Delta Ct}$ method with β-actin, TATA box binding protein, or 18S as endogenous controls.

**Immunoblotting.** Whole-cell lysates were collected as described in *SI Materials and Methods*. Primary antibody incubation was performed overnight at 4 °C with the following antibodies: EDI3 polyclonal antibody (Peptide Specialty Labs, 1:100 or Sigma Prestige, HPA039556, 1:500); phospho-c-Jun, c-Jun, p38 (Santa Cruz Biotechnology; 1:500); β-actin (Sigma; 1:5,000); all other primary antibodies were acquired from Cell Signaling, and used at a dilution of 1:1,000. To detect antibody binding, HRP-conjugated secondary antibodies were used as follows: goat anti-rabbit IgG1 (Cell Signaling; 1:1,000), anti-mouse IgG (Sigma; 1:10,000). All images were taken on a Vilber Fusion Fx7 imager (Vilber Lourmat) and bands quantified using ImageJ (National Institutes of Health).

**RNA Interference.** Three Stealth RNAi siRNA oligos specific for EDI3 and validated Stealth RNAi for PRKCA (cat. no. PRKCAVHS41564) were purchased from Invitrogen and experiments performed according to the manufacturer's instructions as described in *SI Materials and Methods*. Stealth RNAi siRNA Negative Control Med GC (Invitrogen) was used to control for nontargeting effects of the RNAi process.

**EDI3 Activity Assay.** Activity was measured using an enzyme-coupled spectrophotometric assay, adapted from Invitrogen's Amplex Red (10-acetyl-3,7-dihydrophenoxazine) PLD Assay and described in *SI Materials and Methods*. Fluorescence was detected using a SpectraFluor Plus microplate reader (Tecan).

**NMR Spectroscopy.** ***$^{31}$P NMR.*** Either 20 μg recombinant EDI3 protein (AMS Bio) or 250 μg cytoplasm-enriched protein was incubated at 37 °C with 5 mM GPC (Sigma) for the times indicated. The reaction was stopped by snap-freezing in liquid nitrogen and stored at −80 °C until analysis. $^{31}$P spectra were measured at a frequency of 202.49 MHz. Measurements were performed at 7 °C to reduce the amount of sample decomposition during the measurement. Standards predicted the GPC signal at 0.6 ppm and an inorganic phosphate (Pi) signal at 2.6 ppm.

***$^{1}$H NMR.*** Cells were washed twice in cold 1× PBS, incubated for 2 min with cold MeOH, and collected in the MeOH. After centrifugation at 500 × *g* for 5 min, most of the MeOH were removed without disturbing the pellet, and the remaining MeOH left to evaporate overnight. The remaining pellet was stored at −80 °C until analysis. The subsequent sample preparation and $^{1}$H NMR spectroscopy was carried out according to standard procedures (41), and detailed methods are provided in *SI Materials and Methods*.

**Lipid Analysis.** Seventy-two hours after transfection with scrambled or EDI3 siRNA, cells were washed once and collected in ice-cold 1× PBS by scraping. The supernatant was removed following a centrifugation step of 1,700 × *g*, and the pellet resuspended in 1× PBS. Cells were sonicated three times for 10 s, and protein concentration determined using a BCA protein assay kit (Thermo Scientific). Next, 300 μg protein was resuspended in 1 mL 1× PBS and stored at −80 °C until analysis. Lipid analysis in the presence of isotopic labeled or not naturally occurring lipid species as internal standards was

performed as described previously (42, 43). Detailed methods are provided in *SI Materials and Methods*.

**In Vitro Scratch Assay.** An ~400-μm scratch was made using a sterile pipette tip on a fully confluent cell monolayer either 72 h after transfection with siRNA oligos or 24 h after plating MCF7 cells stably overexpressing EDI3 ($1 \times 10^6$ cells per well of a six-well plate). Cells were washed and either replaced with normal culture media or media containing one of the following compounds for the duration of the experiment as described in the respective figure legends: Gö6976 (Calbiochem); TPA (Sigma), Sildenafil (Sigma), and Dipyridamole (Sigma). Images were taken using a phase contrast Eclipse T5100 microscope (Nikon) at the indicated times.

**In Vitro Migration Assay.** Cell motility was assessed using a modified Boyden chamber assay. In brief, $5 \times 10^4$ cells in 250 μL sera-free media were seeded in an upper chamber of a noncoated Transwell insert (24-well insert; pore size, 8.0 μm; BD Biosciences). Media supplemented with serum was used as the chemoattractant in the lower chamber. After 24-h incubation, cells in the upper chamber were removed with a cotton swab and cells which migrated through the pores were fixed and stained with Giemsa (Merck). Images of migrated cells were taken with a phase contrast Eclipse T5100 microscope (Nikon) and number of cells migrated were quantified with ImageJ (National Institutes of Health).

**Statistical Analysis.** For clinical data, Kaplan–Meier curves were plotted to assess overall survival. Different survival curves were compared using the log-rank test. The proportional hazards model was applied to examine whether EDI3 was an independent prognostic factor (univariable and multivariable analyses) (44, 45). The proportional hazards assumption was tested by Cox–Snell residuals showing a good fit of all Cox analysis presented in the results section. A difference between two independent groups was tested by the Mann–Whitney test. Statistical analysis was performed using SPSS 18 software. To analyze the influence of EDI3 knockdown on lipid species, the *t* test or Wilcoxon tests (two-sided) were used depending on whether or not the lipid species showed normal distribution. Student's paired *t* test (two-tailed) was used to compare the difference between two groups where $P < 0.05$ was considered significant.

**ACKNOWLEDGMENTS.** We thank Dr. Silvia Selinski (Technische Universität, Dortmund) for statistical analyses, and Brigitte Begher-Tibbe and Doreen Werchau for technical support. We also thank Gabriel Valbuena and Shyam Solanki (Imperial College London) for support with NMR analyses. This study was supported by the European Union Seventh Framework Programme (FP7)-Health-Projects CancerSys (223188), LipidomicNET (202272) and DETECTIVE (266838) and the BMBF (German Federal Ministry of Education and Research) projects OncoProfile, Virtual Liver, and SysMBo. C.-H.L. was funded by an EPSRC (Engineering and Physical Sciences Research Council) Centre for Doctoral Training Studentship from the Institute of Chemical Biology (Imperial College, London) awarded to H.C.K.

1. Aboagye EO, Bhujwalla ZM (1999) Malignant transformation alters membrane choline phospholipid metabolism of human mammary epithelial cells. *Cancer Res* 59: 80–84.
2. Ackerstaff E, Glunde K, Bhujwalla ZM (2003) Choline phospholipid metabolism: A target in cancer cells? *J Cell Biochem* 90:525–533.
3. Glunde K, Jie C, Bhujwalla ZM (2004) Molecular causes of the aberrant choline phospholipid metabolism in breast cancer. *Cancer Res* 64:4270–4276.
4. Iorio E, et al. (2005) Alterations of choline phospholipid metabolism in ovarian tumor progression. *Cancer Res* 65:9369–9376.
5. Gillies RJ, Morse DL (2005) In vivo magnetic resonance spectroscopy in cancer. *Annu Rev Biomed Eng* 7:287–326.
6. Glunde K, Artemov D, Penet MF, Jacobs MA, Bhujwalla ZM (2010) Magnetic resonance spectroscopy in metabolic and molecular imaging and diagnosis of cancer. *Chem Rev* 110:3043–3059.
7. Iorio E, et al. (2010) Activation of phosphatidylcholine cycle enzymes in human epithelial ovarian cancer cells. *Cancer Res* 70:2126–2135.
8. Negendank W (1992) Studies of human tumors by MRS: A review. *NMR Biomed* 5: 303–324.
9. Podo F (1999) Tumour phospholipid metabolism. *NMR Biomed* 12:413–439.
10. Eliyahu G, Kreizman T, Degani H (2007) Phosphocholine as a biomarker of breast cancer: Molecular and biochemical studies. *Int J Cancer* 120:1721–1730.
11. Ramírez de Molina A, et al. (2002) Increased choline kinase activity in human breast carcinomas: Clinical evidence for a potential novel antitumor strategy. *Oncogene* 21: 4317–4322.
12. Ramírez de Molina A, et al. (2002) Overexpression of choline kinase is a frequent feature in human tumor-derived cell lines and in lung, prostate, and colorectal human cancers. *Biochem Biophys Res Commun* 296:580–583.
13. Hernández-Alcoceba R, Fernández F, Lacal JC (1999) In vivo antitumor activity of choline kinase inhibitors: A novel target for anticancer drug discovery. *Cancer Res* 59: 3112–3118.
14. Katz-Brull R, Degani H (1996) Kinetics of choline transport and phosphorylation in human breast cancer cells; NMR application of the zero trans method. *Anticancer Res* 16(3B):1375–1380.
15. Kouji H, et al. (2009) Molecular and functional characterization of choline transporter in human colon carcinoma HT-29 cells. *Arch Biochem Biophys* 483:90–98.
16. Noh DY, et al. (2000) Overexpression of phospholipase D1 in human breast cancer tissues. *Cancer Lett* 161:207–214.
17. Zhong M, et al. (2003) Phospholipase D prevents apoptosis in v-Src-transformed rat fibroblasts and MDA-MB-231 breast cancer cells. *Biochem Biophys Res Commun* 302: 615–619.
18. Guthridge CJ, Stampfer MR, Clark MA, Steiner MR (1994) Phospholipases A2 in ras-transformed and immortalized human mammary epithelial cells. *Cancer Lett* 86: 11–21.
19. Yamashita S, Yamashita J, Ogawa M (1994) Overexpression of group II phospholipase A2 in human breast cancer tissues is closely associated with their malignant potency. *Br J Cancer* 69:1166–1170.
20. Yanaka N (2007) Mammalian glycerophosphodiester phosphodiesterases. *Biosci Biotechnol Biochem* 71:1811–1818.
21. Okazaki Y, et al. (2010) A novel glycerophosphodiester phosphodiesterase, GDE5, controls skeletal muscle development via a non-enzymatic mechanism. *J Biol Chem* 285:27652–27663.
22. Gallazzini M, Ferraris JD, Burg MB (2008) GDPD5 is a glycerophosphocholine phosphodiesterase that osmotically regulates the osmoprotective organic osmolyte GPC. *Proc Natl Acad Sci USA* 105:11026–11031.
23. Cao MD, et al. (2012) Glycerophosphodiester phosphodiesterase domain containing 5 (GDPD5) expression correlates with malignant choline phospholipid metabolite profiles in human breast cancer. *NMR Biomed*, 10.1002/nbm2766.
24. Hanahan D, Weinberg RA (2011) Hallmarks of cancer: The next generation. *Cell* 144: 646–674.
25. Wang P, et al. (2001) Characterization of human, dog and rabbit corpus cavernosum type 5 phosphodiesterases. *Life Sci* 68:1977–1987.
26. Yalcin A, et al. (2010) Selective inhibition of choline kinase simultaneously attenuates MAPK and PI3K/AKT signaling. *Oncogene* 29:139–149.
27. Exton JH (1990) Signaling through phosphatidylcholine breakdown. *J Biol Chem* 265: 1–4.
28. Kam Y, Exton JH (2004) Role of phospholipase D1 in the regulation of mTOR activity by lysophosphatidic acid. *FASEB J* 18:311–319.
29. Kang DW, et al. (2008) Phorbol ester up-regulates phospholipase D1 but not phospholipase D2 expression through a PKC/Ras/ERK/NFkappaB-dependent pathway and enhances matrix metalloproteinase-9 secretion in colon cancer cells. *J Biol Chem* 283: 4094–4104.
30. Kang DW, et al. (2011) Autoregulation of phospholipase D activity is coupled to selective induction of phospholipase D1 expression to promote invasion of breast cancer cells. *Int J Cancer* 128:805–816.
31. Mills GB, Moolenaar WH (2003) The emerging role of lysophosphatidic acid in cancer. *Nat Rev Cancer* 3:582–591.
32. Nishizuka Y (1992) Intracellular signaling by hydrolysis of phospholipids and activation of protein kinase C. *Science* 258:607–614.
33. Scott SA, et al. (2009) Design of isoform-selective phospholipase D inhibitors that modulate cancer cell invasiveness. *Nat Chem Biol* 5:108–117.
34. Narayan P, Dahiya R (1991) Alterations in sphingomyelin and fatty acids in human benign prostatic hyperplasia and prostatic cancer. *Biomed Biochim Acta* 50: 1099–1108.
35. Foster DA (2009) Phosphatidic acid signaling to mTOR: Signals for the survival of human cancer cells. *Biochim Biophys Acta* 1791:949–955.
36. Cheng CY, et al. (2009) IL-1 beta induces urokinase-plasminogen activator expression and cell migration through PKC alpha, JNK1/2, and NF-kappaB in A549 cells. *J Cell Physiol* 219:183–193.
37. Guo J, et al. (2008) Nicotine promotes mammary tumor migration via a signaling cascade involving protein kinase C and CDC42. *Cancer Res* 68:8473–8481.
38. Ng T, et al. (1999) PKCalpha regulates beta1 integrin-dependent cell motility through association and control of integrin traffic. *EMBO J* 18:3909–3923.
39. American Cancer Society (2010) *Cancer Facts and Figures 2010* (American Cancer Society, Atlanta).
40. Steiner E, et al. (2003) Multivariate independent prognostic factors in endometrial carcinoma: A clinicopathologic study in 181 patients: 10 years experience at the Department of Obstetrics and Gynecology of the Mainz University. *Int J Gynecol Cancer* 13:197–203.
41. Keun HC, Athersuch TJ (2011) Nuclear magnetic resonance (NMR)-based metabolomics. *Methods Mol Biol* 708:321–334.
42. Ecker J, et al. (2010) Induction of fatty acid synthesis is a key requirement for phagocytic differentiation of human monocytes. *Proc Natl Acad Sci USA* 107: 7817–7822.
43. Leidl K, Liebisch G, Richter D, Schmitz G (2008) Mass spectrometric analysis of lipid species of human circulating blood cells. *Biochim Biophys Acta* 1781:655–664.
44. Micke P, et al. (2003) Characterization of c-kit expression in small cell lung cancer: Prognostic and therapeutic implications. *Clin Cancer Res* 9:188–194.
45. Micke P, et al. (2001) c-erbB-2 expression in small-cell lung cancer is associated with poor prognosis. *Int J Cancer* 92:474–479.